# Tunable fly's-eye lens made of patterned polymer-dispersed liquid crystal

**Y. J. Liu, X. W. Sun*, and P. Shum**

*School of Electrical and Electronic Engineering, Nanyang Technological University, Nanyang Avenue, Singapore 639798*
*exwsun@ntu.edu.sg*

**X. J. Yin**

*School of Chemical & Life Sciences, Display Technology Center, Singapore Polytechnic 500 Dover Road, Singapore 139651*

**Abstract:** A fly's-eye lens was fabricated using polymer-dispersed liquid crystals and its optical properties were evaluated. The morphologies were examined under an optical microscope. The forming process has been simulated based on a patterned photo-polymerization technique in which the spatially modulated reaction rate has been coupled with the time-dependent Ginzburg-Landau (TDGL) equations with the free energies relating to isotropic mixing, nematic ordering, and network elasticity incorporated. The simulated results are in good agreement with the experimental results. The beam profile was tested using a CCD. The results showed that this fly's-eye lens could modulate a Gaussian beam into a mesa-like beam. Such device is potentially useful in beam shaping and many illumination systems that require uniform beam profile.



**OCIS codes:** (080.3630) Lenses; (230.3720) Liquid-crystal devices; (160.5470) Polymers.

## References and links

1. C. -M. Chang, and H. -P. D. Shieh, "Design of illumination and projection optics for projectors with single digital micromirror devices," Appl. Opt. **39**, 3202-3208 (2000).
2. B. G. Crowther, D. G. Koch, J. M. Kunick, J. P. McGuire, R. Harned, and R. Gotin, "A fly's eye condenser system for uniform illumination," Proc. SPIE **4832**, 302-310 (2002).
3. A. H. J. van den Brandt, and W. A. G. Timmers, US Patent 5, 098, 184 (1990).
4. Y. Masumoto,US Patent 5, 418, 583 (1993).
5. H. Shimonura, Y. Manabe, T. Hattori, M. Kusano, and A. Sekine, US Patent 5, 959, 778 (1997).
6. M. Foley, and J. Munro, "Polymer fly's eye light integrator lens arrays for digital projectors," SID Symposium Digest **31**, 870-873 (2000).
7. M. Foley, "Technical advances in microstructured plastic optics for display applications," SID Symposium Digest **30**, 1106-1109 (1999).
8. J. W. Doane, N. Z. Vaz, and B. -G. Wu, S. Zumer, "Field controlled light scattering from nematic microdroplets," Appl. Phys. Lett. **48**, 269-271 (1986).
9. Y. J. Liu, X. W. Sun, J. H. Liu, H. T. Dai, and K. S. Xu, "A polarization insensitive $2 \times 2$ optical switch fabricated by liquid crystal-polymer composite," Appl. Phys. Lett. **86**, 041115 (2005).
10. R. L. Sutherland, L. V. Natarajan, V. P. Tondiglia, S. A. Siwecki, S. Chandra, and T. J. Bunning, "Switchable holograms for displays and telecommunications," Proc. SPIE **4463**, 1-10 (2001).
11. V. P. Tondiglia, L. V. Natarajan, R. L. Sutherland, T. J. Bunning, and W. W. Adams, "Volume holographic image storage and electro-optical readout in a polymer-dispersed liquid-crystal film," Opt. Lett. **20**, 1325-1327 (1995).
12. H. Yuan, J. Colegrove, G. Hu, T. Fiske, A. Lewis, J.Gunther, L. Silverstein, C. Bowley, G. Crawford, L. Chien, and J. Kelly, "HPDLC color reflective displays," Proc. SPIE **3690**, 196-206 (1999).
13. C. C. Bowley, A. K. Fontecchio, G. P. Crawford, J.-J. Lin, L. Li, and S. Faris, "Multiple gratings simultaneously formed in holographic polymer-dispersed liquid-crystal displays," Appl. Phys. Lett. **76**, 523-525 (2000).
14. Y. J. Liu, B. Zhang, Y. Jia, and K. S. Xu, "Improvement of the diffraction efficiency in holographic polymer dispersed liquid crystal Bragg gratings," Opt. Commun. **218**, 27-32 (2003).

#69628 - $15.00 USD Received 3 April 2006; revised 9 May 2006; accepted 11 May 2006

15. J. R. Dorgan, and D. Yan, "Kinetics of spinodal decomposition in liquid crystalline polymers: processing effects on the phase separation morphology," Macromolecules **31**, 193-200 (1998).
16. D. Nwabunma, and T. Kyu, "Phase behavior of mixtures of low molar mass nematic liquid crystal and in situ photo-cross-linked polymer network," Macromolecules **32**, 664-674 (1999).
17. D. Nwabunma, H.-W. Chiu, and T. Kyu, "Theoretical investigation on dynamics of photopolymerization-induced phase separation and morphology development in nematic liquid crystal/polymer mixtures," J. Chem. Phys. **113**, 6429-6436 (2000).
18. T. Kyu, and D. Nwabunma, "Simulations of microlens arrays formed by pattern-photoplymerization-induced phase separation of liquid crystal/monomer mixtures," Macromolecules **34**, 9168-9172 (2001).

## 1. Introduction

Irradiance uniformity is a prerequisite in many optical projection systems. Light sources rarely produce the required uniformity for most simple illumination systems. Therefore, some modification of the irradiance pattern produced by the light source is a necessity. The optical systems used to accomplish this goal generally apply flux integration scheme. Rod integrators and fly's-eye integrator arrays are typically employed to convert the bulb filament - a point or tiny line - into homogeneous illumination, for example, over an array of liquid crystal light-valves in liquid crystal display (LCD) projector [1 - 5]. However, the rod-type integrators are physically long and heavy, and optically slow, which is fundamentally incompatible with today's trend toward smaller, lighter projectors. Fly's-eye integrators are more compatible with this trend. A typical characteristic of such high throughput integrators is that they can produce a discontinuous pupil irradiance distribution and a condenser lens is used to make the pupil irradiance optically overlapped at the illumination plane to achieve a uniform light from a nonuniform source. Traditionally, fly's-eye integrators have been made from molded glass. Glass is popular because it has good temperature resistance and mechanical properties, and its performance is well understood now.

Polymer fly's-eye lens integrators are also available now, and have been included in numerous front and rear LCD projector applications [6]. These lenses have been fabricated from acrylic (PMMA), polycarbonate (PC), and various high temperature thermoplastics with high precision molding process [7]. The potential advantages of a plastic light integrator in comparison with glass are lighter weight, lower cost, and better performance (higher transmissivity and overall uniformity). However, resistance of plastic to continuous, high operating temperatures and birefringence in plastic parts are still key concerns. These problems limit their applications to a great extent.

Polymer-dispersed liquid crystal (PDLC) has been studied for about twenty years since it was firstly reported by Doane and his co-workers [8]. It holds promise for many applications ranging from switchable windows to projection displays. The combination with holography makes holographic polymer-dispersed liquid crystal (H-PDLC) more useful in optical communications [9, 10], information storage [11], integrated optics and flat panel displays [12, 13]. The most interesting thing in PDLCs and H-PDLCs is that liquid crystals exist in the form of droplets, and the liquid crystal director can be reoreintated by applying a voltage. The refractive index difference between liquid crystal droplets and polymer matrix can change the phase of the incoming light and cause the light being scattered or transmitted in PDLCs and diffracted or transmitted in H-PDLCs. Based on this concept and laser patterning technique, a tunable fly's-eye lens fabricated with PDLC shall be reported in this paper. The forming process has been simulated based on a patterned photo-polymerization technique in which the spatially modulated photoreaction rate is coupled with the time-dependent Ginzburg-Landau (TDGL) equations by incorporating free energy densities of isotropic mixing, nematic ordering, and network elasticity. The simulated morphologies were very similar to what we obtained experimentally. Its optical properties were examined and the results showed that the tunable PDLC fly's-eye lens could be a potential alternative to conventional glass fly's-eye lens.

#69628 - $15.00 USD Received 3 April 2006; revised 9 May 2006; accepted 11 May 2006

## 2. Experiment

Figure 1 shows the experimental setup to fabricate the fly's-eye lens. The key element is a fly's-eye lens mask (LIMO, Germany) of about 3.5 × 3.5 $cm^2$ in size, which produces a periodical dot array pattern at its focal plane. This pattern is then minimized using a large aperture lens, which has an effective focal length of 150 mm. The minimized pattern is about 0.7 × 0.7 $cm^2$ at the focal plane of the lens. A LC cell filled with prepolymer/LC mixture is placed on the focal plane of $L_3$ to record this pattern. During exposure, in the area with higher exposure intensity, absorption by the photoinitiator results in a highly reactive triplet state. The coinitiator undergoes an electron-transfer reaction with this triplet state to create a free radical. Free-radical polymerization is then initiated. Hence, spatial gradients in the chemical potential are established which produces a diffusion of monomers (and other reactants) into the bright regions, and a counter-diffusion of LCs into the dark regions. This process continues until a new equilibrium chemical potential is established. Finally, a phase type fly's-eye lens with periodical gradient refractive index is formed in the PDLC cell. When a voltage is applied on the cell, the liquid crystal molecules will reorientate along the direction of the electric field. If the refractive indices of polymer matrix and LC are matched, the light beam will pass through directly as if it is a homogeneous film. So a laser beam can be tuned from a uniform to Gaussian distribution. This may be useful in beam shaping and also potentially useful in many illumination systems that require uniform beam profile.

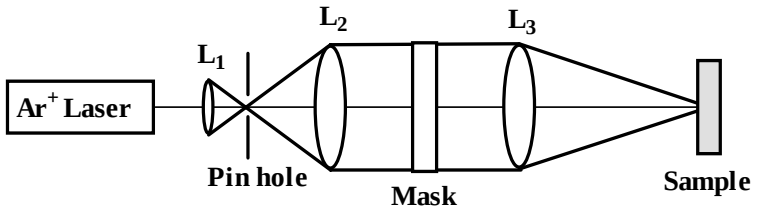


Fig. 1. The experimental setup to fabricate the PDLC fly's-eye lens. $L_1$, $L_2$ and $L_3$ are all lenses. $L_1$ and $L_2$ are used to generate a collimated laser beam. $L_3$ is used to minimize the pattern.

In this experiment, the materials used to fabricate the fly's-eye lens were monomer, trimethylolpropane triacrylate (TMPTA); cross-linking monomer, N-vinylpyrrollidone (NVP); surfactant, octanoic acid (OA); coinitiator, N-phenylglycine (NPG); and photoinitiator, rose bengal (RB); all from Aldrich. In prepolymer, the ratio of TMPTA/NVP/OA/NPG/RB was 62/25/10/2/1 by weight [14]. The LC used was E7 (Merck) with an ordinary refractive index of $n_o$ = 1.521, and a birefringence of $\Delta n$ = 0.225. The prepolymer and LC were mechanically blended in dark conditions according to the appropriate weight ratio at 65 °C (higher than the clearing point of the LC E7) to form a homogeneous mixture. In this prepolymer/LC mixture, the LC concentration was about 35 wt%. A droplet of the mixture was sandwiched between two pieces of indium tin oxide (ITO) coated glass. The cell gap was about 30 μm. The curing intensity before the photomask was 12 $mW/cm^2$ and the exposure time was 120 s. After exposure, the samples were further cured for 5 mins using a UV lamp to ensure the complete polymerization of the prepolymer. All samples were measured with a 543 nm He-Ne laser at room temperature. For morphology analysis by optical microscope, the test samples were broken with the ITO glass on one side removed, soaked in ethanol for more than 12 hrs to remove LC, and finally dried.

## 3. Morphological Simulations

The photopatterning process of the LC microlens can be modeled by mimicking spatiotemporal growth of concentration and orientation order parameters of the LC in which a photoreaction rate equation is coupled with the TDGL model, as described below: [15 – 18]

#69628 - $15.00 USD Received 3 April 2006; revised 9 May 2006; accepted 11 May 2006

$$\frac{\partial \phi_M}{\partial t} = \nabla \bullet \left[ \Lambda \nabla \frac{\partial G}{\partial \phi_M} \right] + \eta_{\phi M} \quad \text{or} \quad \frac{\partial \phi_P}{\partial t} = \nabla \bullet \left[ \Lambda \nabla \frac{\partial G}{\partial \phi_P} \right] + \eta_{\phi P} \tag{1}$$

$$\frac{\partial \phi_L}{\partial t} = \nabla \bullet \left[ \Lambda \nabla \frac{\partial G}{\partial \phi_L} \right] + \eta_{\phi L} \tag{2}$$

$$\frac{\partial S}{\partial t} = \nabla \bullet \left[ \Lambda \nabla \frac{\partial G}{\partial S} \right] + \eta_S \tag{3}$$

where $\phi_M(r,t)$ and $\phi_P(r,t)$ are the monomer and emerging polymer concentrations, respectively, $\phi_L(r,t)$ is the conserved concentration (volume fraction) order parameter of LC at position *r* and time *t*, $S(r,t)$ is the nonconserved orientational order parameter of LC at the same position and time, $G(r,t)$ is the total free energy of the system, $\Lambda$ is the mutual translational diffusion coefficient, $\eta_{\phi M}(r,t)$, $\eta_{\phi P}(r,t)$ and $\eta_{\phi L}(r,t)$ are the noise terms which represent the concentration fluctuations of monomer, polymer and LC, respectively, and $\eta_S(r,t)$ is the orientation fluctuations of the LC directors that satisfy the fluctuation dissipation theorem.

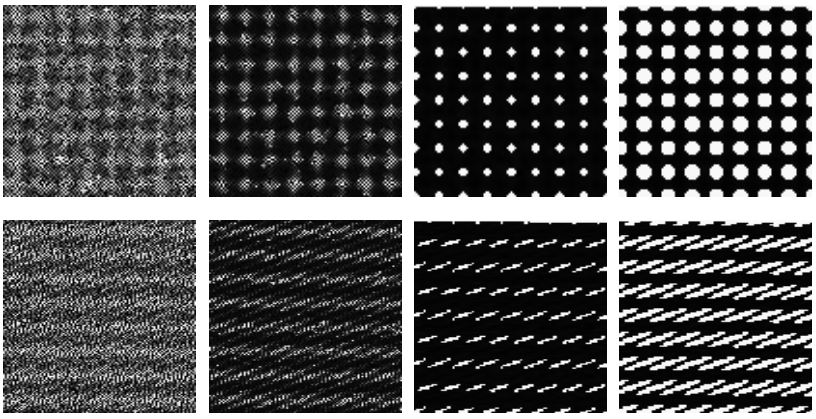

Fig. 2. The evolution of a hypothetical patterned PDLC fly's-eye lens showing the array patterns. Parameters used were $\phi_L = 0.75$, $T = 30°\text{C}$, $k_0 = 10^{-4}$, $I_0 = 1.0$. The upper row shows the case for $N_x = N_y = 100$, while the lower row represents that for $N_x = 100$, and $N_y = 150$.

It can be predicted that polymerization occurs preferentially in the high-intensity regions due to the fast photoreaction rate that causes LC molecules diffuse into the low-intensity regions and form droplets. Fig. 2 demonstrates the time sequence of the spatiotemporal development of microlens arrays calculated using the parameters: $\phi_L = 0.75$, $T = 30°\text{C}$, $k_0 = 10^{-4}$, $I_0 = 1.0$, where *T* is the reaction temperature, $k_0$ is the reaction rate constant, $I_0$ is the exposure intensity. The upper row shows the emerging patterns in the compositional order parameter field for $N_x = N_y = 100$, while the lower row represents those with $N_x = 100$, and $N_y = 150$. Here, $N_x$ and $N_y$ represent the number of elements, related to the periodicity in the horizontal and vertical directions, respectively. In the simulation, one can envisage the emergence of microlens with varying shapes, *viz* spherical or elliptical as depicted in Fig. 2. As seen in the upper row figure, the light pattern gives rise to the array of spherical microlens when $N_x = N_y$. However, when $N_x \neq N_y$, the elliptical microlens arrays (lower row) may be

#69628 - $15.00 USD Received 3 April 2006; revised 9 May 2006; accepted 11 May 2006

obtained. Therefore, the microlens with different shapes was obtained by controlling the light pattern, i.e. $N_x$ and $N_y$.

The surface morphologies of the samples were observed under an optical microscope. Figure 3(a), (b) and (c) show the micrographs of the fly's-eye lens at different microregions. The bright and dark regions are polymer-rich and LC-rich regions, respectively. It can be seen from Fig. 3 that, the morphologies are very similar to the theoretical simulations. However, because of the aberration of the lens and the interference among the minimized light beams, the morphologies of the fly's-eye lens in different microregions are very different. Here, we only showed three typical morphologies obtained. Judging from the experimental results in the following part, this morphological difference doesn't influence the performance of the fly's-eye lens.

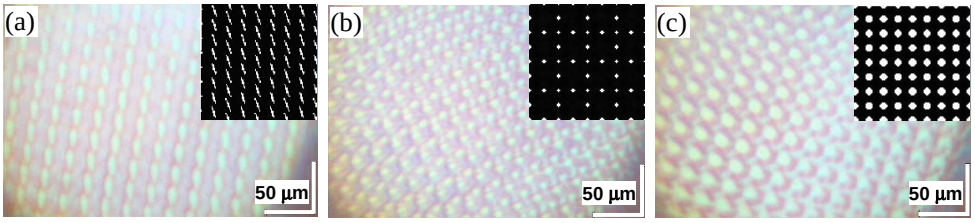


Fig. 3. The micrographs (a), (b), and (c) are obtained under the optical microscope. The insets are the theoretical simulations, which show the similar morphologies.

## 4. Results and discussion

Figure 4(a) shows the overall morphologies of the fly's-eye lens. By doing the Fourier transform of the micrograph, we obtained the far field pattern as shown in Fig. 4(b). It can be seen that when a collimated light beam is incident on the fly's-eye lens, many bright spots can be obtained at the far field. The recorded pattern divides the incoming light into many beams and then these beams can interfere with each other. As a result, when a laser beam was incident on the fly's-eye lens, it can be expanded into a beam with uniform intensity. In our experiment, the incoming laser beam was about 0.8 mm in diameter with Gaussian distribution in intensity. After passing through the fly's-eye lens, the expanded beam was about 4 mm in diameter with uniform distribution in intensity at the distance of about 10 mm from the fly's-eye lens.

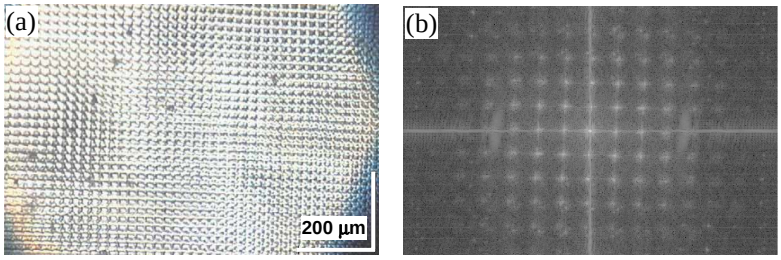


Fig. 4. The overall micrograph of the patterned PDLC fly's-eye lens, (a), and its Fourier transform pattern, (b).

Figure 5(a) and (b) show the near and far field patterns of the PDLC fly's-eye lens, respectively. Fig. 5(a) was obtained using a CCD 10 mm away from the fly's-eye lens when the He-Ne laser beam passed through the sample. It showed roundly even brightness except the saw-like pattern at the circle edge. When the beam propagates further along the optical

#69628 - $15.00 USD Received 3 April 2006; revised 9 May 2006; accepted 11 May 2006

path, the light beam would divide into many light dots, as shown in Fig. 5(b). This result was in good agreement with the Fourier analysis of the micrograph of the fly's-eye lens, as shown in Fig. 4(b).

To check the intensity distribution, the intensities of the incoming and output light were examined using a CCD. Figure 6(a), (b) and (c) show the intensity distribution of the incoming light, the output light with no voltage and the output light with voltage applied, respectively. It can be seen from Fig. 6, the incoming light is a typical Gaussian distribution, as indicted in Fig. 6(a). With no voltage applied on the cell, the output light was modulated into a beam with an approximately flat intensity distribution, as shown in Fig. 6(b). With an applied voltage of about 300 V, i.e. 10 V/μm, the light intensity distribution was recovered to a Gaussian-like beam, as shown in Fig. 6(c), although it seemed not perfect. Therefore, a Gaussian laser beam can be modulated into a mesa-like beam by such a PDLC fly's-eye lens. It is worth mentioning that the applied voltage was a square wave and the switching time was about 50 ms.

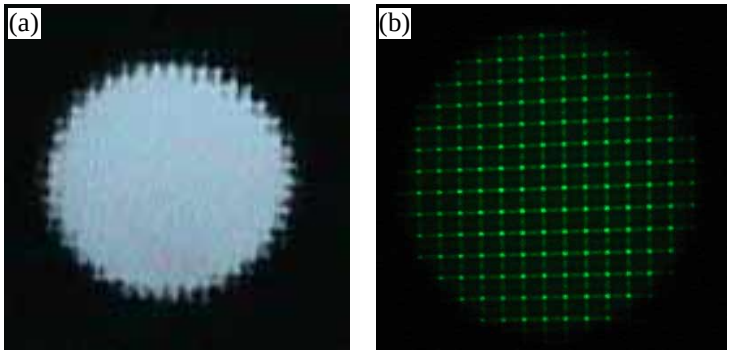


Fig. 5. The near field (a) and far field (b) patterns of the fly's-eye lens, which are obtained by a CCD 10 mm and 20 cm away from the fly's-eye lens when the laser beam passes through it, respectively.

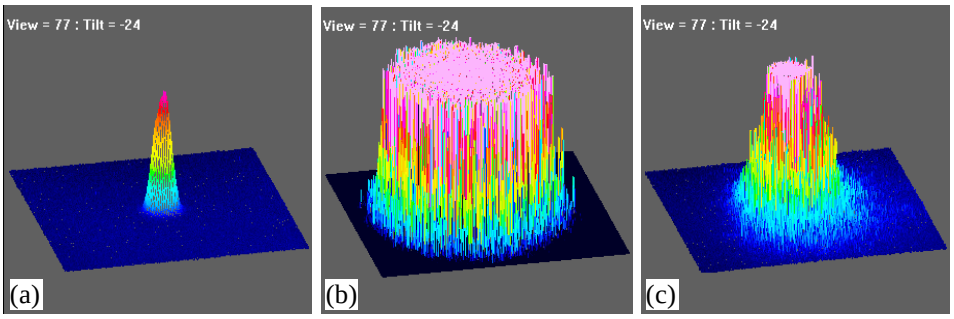


Fig. 6. The intensity distribution of the incoming light (a), the output light without voltage (b), and with voltage applied (c), respectively.

In comparison with conventional glass fly's-eye lens, the major advantages of such fly's-eye lens are easy fabrication process, compactness, light weight and low cost. It is a flat device, indicating a simpler fabrication process than the polymer fly's-eye lens. Moreover, PDLC fly's-eye lens is electrically tunable. However, it also shares the same drawbacks with the polymer fly's-eye lens and has poorer temperature resistance because LC can only work in relatively small temperature range.

#69628 - $15.00 USD Received 3 April 2006; revised 9 May 2006; accepted 11 May 2006

## 5. Conclusion

In conclusion, an electrically tunable fly's-eye lens was fabricated using patterned PDLC. It showed easy fabrication and good optical properties. The theoretical simulation showed that it could provide a good guide to control the morphologies of the recorded pattern. The fly's-eye lens can modulate a Gaussian laser beam into a mesa-like beam. Such a fly's-eye lens is potentially useful in beam shaping and low intensity optical illumination systems.

#69628 - $15.00 USD Received 3 April 2006; revised 9 May 2006; accepted 11 May 2006